ELSEVIER

Journal of Power Sources 81–82 (1999) 777–781

JOURNAL OF POWER SOURCES

www.elsevier.com/locate/jpowsour

Lithium ion conductivity of A-site deficient perovskite solid solutions

Yasuhiro Harada, Hiroyuki Watanabe, Jun Kuwano *, Yasukazu Saito

Department of Industrial Chemistry, Faculty of Engineering, Science University of Tokyo, 1-3 Kagurazaka, Shinjuku-ku, Tokyo 162-8601, Japan

Abstract

Over twenty of A-site deficient perovskite solid solution with Li^+ ion conductivity (Li-ADPESSs) were prepared with the M and Li concentration fixed at $M_{0.56}Li_{0.33}TiO_3$ in the five series: (A) $(La_{1-X}Nd_X)_{0.56}Li_{0.33}TiO_3$, (B) $La_{0.56}Li_{0.33}M(IV)_XTi_{1-X}O_3$[M(IV) = Zr,Hf], (C) $(Ca_{1-X}Sr_X)_{0.56}Li_{0.33}Ta_{0.56}Ti_{0.44}O_3$, (D) $(Ca_{1-X}Sr_X)_{0.56}Li_{0.33}Fe_{0.225}Ta_{0.775}O_3$, E) $Sr_{0.56}Li_{0.33}M(|||)_{0.225}Ta_{0.775}O_3$[M(|||) = Cr,Fe,Co,Ga,Y]. Except for the few, the quenched samples were the α-form with disordered arrangement of the A-site ions. The relation between bulk conductivity (σ_b) and the cube root ($V^{1/3}$) of the perovskite cell volume showed a maximum at $V^{1/3} \approx 387$ pm for the series A, B and at $V^{1/3} \approx 395$ pm for the series C–E, respectively. The perovskite framework containing less covalent, large cations calls for a larger optimal cell volume for fast conduction.

Keywords: Ionic conductivity; Lithium ion; Perovskite; Solid solution; Solid electrolyte; A-site deficient

1. Introduction

Several kinds of *A*-site *D*eficient *Pe*rovskite *S*olid *S*olution with high lithium ion conductivity (Li-ADPESS) have been discovered and the ionic conduction phenomena and crystal chemistry have been extensively investigated in recent years [1–16]. They are titanates except for the few based on tantalates [11] and have neither a loose packing nor open framework unlike β-Al_2O_3 and NASICON, but a close AO_3 packing. The ionic conduction in the Li-ADPESSs is generally believed to occur by an ion-vacancy mechanism through the interconnecting the A-sites [3–5,10]. In comparison with other lithium ion conducting materials with γ_{II}-$LiPO_3$ [17,18] and spinel structures [19], it is unique in that the ionic conduction takes place not via tetrahedral and octahedral sites in a close packing but via the 12 coordinate A-sites forming the close AO_3 packing.

The bulk ionic conductivity (σ_b) in Li-ADPESSs has been found to depend chiefly on the factors described below.

1.1. Degree of ordering [13,14]

In Li-ADPESSs, the highest value of 1.53×10^{-3} S cm^{-1} at 25°C was found in a simple perovskite α-$La_{0.67-X}Li_{3X}TiO_3$ ($a = a_p$) with disordered arrangement of La^{3+} ions. The disordered α-$La_{0.56}Li_{0.33}TiO_3$ underwent an order–disorder (β-to-α) transition at about 1150°C owing to the alternate arrangement of the La^{3+}-rich (Li^+ · vacancy-poor) and -poor (Li^+ · vacancy-rich) layers along the *c*-axis of the superstructure cell ($a \approx a_p$, $c \approx 2a_p$,) [20]. In the low-temperature β-form, the ionic conductivity decreased in spite of the formation of more Li^+ · vacancy-rich layers as the degree of ordering increased with decreasing temperature in a range, 600–1150°C.

1.2. Concentrations of the immobile A-site ions, the Li^+ ions and the vacancies [3–5]

In $La_{0.67-X}\ Li_{3X}TiO_3$, the concentrations of the Li^+ ions and vacancies were optimized at $x \approx 0.11$–0.12, with a conductivity maximum. In a high concentration region of the immobile A-site ions, the conductivity has been considered to be dominated by a percolation phenomenon [15].

1.3. Size of the perovskite cell [5,16]

In β-$(La_{1-X}Nd_X)_{0.56}Li_{0.33}TiO_3$ and β-$Ln_{0.5}Li_{0.5}TiO_3$ (Ln: lanthanides), the ionic conductivity has been reported to increase with increasing ionic radius of Ln^{3+}, namely, the cube root ($V^{1/3}$) of the perovskite cell volume ($V \approx a_p^3$).

In this study, with the M and Li concentrations fixed at $M_{0.56}Li_{0.33}TiO_3$, we prepared more than 20 of ADPESSs (mostly α-form with the disordered arrangement of A-site ions) under almost the same preparation conditions.

* Corresponding author. Tel.: +81-3-3260-4271 ext. 3487; Fax: +81-3-5261-4631; E-mail: j_kuwano@ci.kagu.sut.ac.jp

0378-7753/99/$ - see front matter
PII: S0378-7753(99)00105-6

ADPESSs with a larger cell volume than that of $La_{0.56}Li_{0.33}TiO_3$ were prepared by substituting larger Sr^{2+} ions for the La^{3+} ions because La^{3+} ion is the largest of generally available trivalent ions. The ADPESSs prepared here can be classified into five series of solid solution: (A) $(La_{1-X}Nd_X)_{0.56}Li_{0.33}TiO_3$, (B) $La_{0.56}Li_{0.33}M(IV)_X Ti_{1-X}O_3$[M(IV) = Zr,Hf], (C) $(Ca_{1-X}Sr_X)_{0.56}Li_{0.33}Ta_{0.56}Ti_{0.44}O_3$, (D) $(Ca_{1-X}Sr_X)_{0.56}Li_{0.33}Fe_{0.225}Ta_{0.775}O_3$, (E) $Sr_{0.56}Li_{0.33}M(|||)_{0.225}Ta_{0.775}O_3$ [M(|||) = Cr,Fe, Co,Ga,Y]. We thus examined the relationships between σ_b and $V^{1/3}$ and discussed determining factors for ionic conductivity in Li-ADPESSs.

2. Experimental

Samples were prepared by a conventional solid-state reaction. Reagent grade $CaCO_3$, Co_2O_3, Cr_2O_3, Fe_2O_3, Ga_2O_3, HfO_2, In_2O_3, La_2O_3, Li_2CO_3, Nd_2O_3, $Sr(NO_3)_2$, Ta_2O_5, TiO_2, Y_2O_3, and ZrO_2 (Wako Pure Chemical Ind.) were dried at 140°C for 5 h in a vacuum prior to use, and required amounts of the starting reagents were thoroughly mixed in an agate mortar with a pestle. All the compositions were expressed as (immobile A-site ions)$_{0.56}$ $Li_{0.33}$(B-site ions)$_{1.0}O_3$, divided into the five series: $(La_{1-X}Nd_X)_{0.56}Li_{0.33}TiO_3$; $La_{0.56}Li_{0.33}M(IV)_X Ti_{1-X}O_3$[M(IV) = Zr,Hf]; $(Ca_{1-X}Sr_X)_{0.56}Li_{0.33}Ta_{0.56}Ti_{0.44}O_3$; $(Ca_{1-X}Sr_X)_{0.56}Li_{0.33}In_{0.225}Ta_{0.775}O_3$; $Sr_{0.56}Li_{0.33}M(|||)_{0.225}Ta_{0.775}O_3$ [M(|||) = Cr,Fe,Co,Ga,Y]. The mixtures were heated initially at 650°C for 2 h to expel CO_2 gas and calcined at 800°C for 12 h on Au-boats. The reground products were pressed at 250 MPa into pellets (12 mm in diameter, 1–2 mm in thickness), which were sintered at 1350°C or 1400°C for 1 h on Pt-boats in a covered Al_2O_3 crucible. The pellets were quenched into liquid nitrogen to form samples of the disordered α-form as perfect as possible.

Table 1
Electrical properties and data of crystal chemistry for Li-ADPESSs prepared in this study

Series and compositions	σ_b at 25°C (S cm^{-1})	σ_{total} at 25°C (S cm^{-1})	Phase present	Crystal system	Lattice constant/pm	Remark
(A) $(La_{1-X}Nd_X)_{0.56}Li_{0.33}TiO_3$						
$X = 0$	1.3×10^{-3}	1.2×10^{-5}	α	Cubic	$a = 387.3$	
0.25	2.1×10^{-4}	1.5×10^{-5}	α	Cubic	$a = 386.3$	
0.5	3.6×10^{-5}	5.4×10^{-6}	α	Cubic	$a = 384.8$	
0.75	3.1×10^{-6}	9.1×10^{-7}	β [a]	Tetragonal	$a = 383.2$, $c = 768.6$	$c \approx 2a_P$
1.0	1.3×10^{-6}	$\approx 10^{-8}$	β [a]	Tetragonal	$a = 382.4$, $c = 770.8$	$c \approx 2a_P$
(B) $La_{0.56}Li_{0.33}M(IV)_X Ti_{1-X}O_3$						
M(IV) = Zr $X = 0.05$	3.1×10^{-4}	3.7×10^{-5}	α	Cubic	$a = 388.1$	
0.10	1.2×10^{-4}	7.8×10^{-6}	α	Cubic	$a = 388.7$	
Hf $X = 0.05$	2.7×10^{-4}	3.4×10^{-5}	α	Cubic	$a = 388.2$	
0.10	1.6×10^{-4}	1.9×10^{-5}	α	Cubic	$a = 388.7$	
(C) $(Ca_{1-X}Sr_X)_{0.56}Li_{0.33}Ta_{0.56}Ti_{0.44}O_3$						
$X = 0$	2.2×10^{-11} [c]	–	α	Orthorhombic	$a = 548.7$, $b = 538.1$, $c = 385.7$	$a \approx b \approx \sqrt{2}\,a_P$
0.3	5.7×10^{-10} [c]	–	α	Cubic	$a = 386.0$	
0.5	6.2×10^{-7}	–	α	Cubic	$a = 388.4$	
0.8	1.5×10^{-5}	2.1×10^{-6}	α	Cubic	$a = 391.2$	
1.0	5.6×10^{-4}	3.5×10^{-6}	α	Cubic	$a = 393.8$	
(D) $(Ca_{1-X}Sr_X)_{0.56}Li_{0.33}Fe_{0.225}Ta_{0.775}O_3$						
$X = 0$	1.5×10^{-6} [b]	1.8×10^{-7} [b]	α	Orthorhombic	$a = 552.5$, $b = 539.2$, $c = 386.0$	$a \approx b \approx \sqrt{2}\,a_P$
0.2	5.8×10^{-7}	9.3×10^{-8}	α	Orthorhombic	$a = 553.1$, $b = 543.4$, $c = 387.5$	$a \approx b \approx \sqrt{2}\,a_P$
0.5	4.1×10^{-5}	5.8×10^{-7}	α	Cubic	$a = 390.3$	
0.8	9.8×10^{-5}	6.8×10^{-5}	α	Cubic	$a = 393.5$	
0.9	1.3×10^{-4}	8.2×10^{-6}	α	Cubic	$a = 395.2$	
1.0	See the data of M(|||) = Fe in E)					
(E) $Sr_{0.56}Li_{0.33}M(|||)_{0.225}Ta_{0.775}O_3$						
M(|||) = Cr	1.0×10^{-4}	2.5×10^{-5}	α	Cubic	$a = 394.8$	
Fe	8.5×10^{-5}	4.1×10^{-6}	α	Cubic	$a = 396.1$	
Co	5.1×10^{-6}	8.8×10^{-7}	α	Cubic	$a = 397.8$	
Ga	7.7×10^{-6}	1.4×10^{-7}	α	Cubic	$a = 395.4$	+ Unknown
Y	$< 10^{-9}$	–	α	Tetragonal	$a = 400.0$, $c = 401.4$	

[a] The superstructure lines are so weak that the samples can be regarded as the α-form.
[b] The contribution of electronic conduction was dominant.
[c] Values extrapolated from data above room temperature.

Phases present in the sintered samples were characterized at room temperature by powder X-ray diffraction (XRD) with a Rigaku RAD-C system (Ni-filtered Cu-Kα, Si internal standard) and the Cell-series programs [21].

A conductivity cell was prepared by applying dc-sputtered gold electrodes onto the opposite faces of the sintered pellet polished with successive lapping films. The cell was placed between two outer gold-plate electrodes on a conductivity jig, which was put in a Pyrex tube. The temperature of the cell was regulated within ± 0.1°C in a range of -60°C–$+60$°C by putting the tube in a thermostatted ethylene glycol-water bath with a programmable temperature PID-controller. A tubular electric furnace was used for the temperature control above 60°C. The cell was kept for about 1 h at each temperature to make sure of the temperature equilibrium prior to the start of measurements. The ac–impedance data were collected under a dry argon gas flow with an impedance meter (YHP 4192A) over a frequency range, $f = 5$ Hz–13 MHz, and analyzed by using the complex impedance or admittance diagrams (i.e., Z'–Z'' and Y'–Y'' plots), and the complex impedance and electric modulus spectra (i.e., Z''–f and M''–f plots) [22].

3. Results and discussion

All the compositions prepared in this studies are listed in Table 1, together with their bulk and total conductivities at 25°C, phases present in the sinters, the crystal systems and lattice parameters of the synthesized ADPESSs. They were a single perovskite-related phase except for the composition $Sr_{0.56}Li_{0.33}M(III)_{0.225}Ta_{0.775}O_3$ [M(III) = Ga], which contained an unknown extra phase. Since the amount of the second phase was very small, we use the data for discussion below. On close examination on their XRD patterns, the perovskite-related phases were found to be the α-form [13,14,20] based on the disordered arrangement of the A-site ions, except for $x = 0.75$ and 1.0 in $(La_{1-x}Nd_x)_{0.56}Li_{0.33}TiO_3$. Both compositions showed very weak superstructure lines due to the β-from [13,20]. We thus regard that both have almost the same properties as the corresponding samples of α, because the degrees of ordering were very low. With reference to superstructures based on other orderings of the A-site ions, no forms other than the β-form were found in all the compositions.

An ADPESS formed over the whole range of the series of A, C and D, whereas the formation ranges were limited to $x = 0$–0.1 in the series B. The tolerance factor, t, for all the listed compositions ranges from $t = 0.948$ for $Nd_{0.56}Li_{0.33}TiO_3$ to $t = 0.999$ for $Sr_{0.56}Li_{0.33}Ta_{0.56}Ti_{0.44}O_3$. Distortion of the primitive perovskite cell took place with six compositions, of which t values were smaller than about 0.964: $x = 0.75$, 1.0 in the series A; $x = 0$ in the series C; $x = 0$, 0.2 in the series D; M(III) = Y in the series E.

The bulk conductivities at 25°C of all the Li-ADPESSs prepared here are plotted against $V^{1/3}$ in Fig. 1.

Series A: As a whole, the dependence of σ_b on $V^{1/3}$ value for the series A was consistent with those reported for the same series of β-form [5] and for β-$Ln_{0.5}Li_{0.5}TiO_3$ [16]. With decreasing $V^{1/3}$ value, the logarithm of σ_b decreased linearly in a range $x = 0$–0.5 and more steeply in a range of $x > 0.5$ as the perovskite cell was distorted.

Series B: Since La^{3+} ions are the largest of generally available trivalent ions, we substitute Zr^{4+} and Hf^{4+} ions for Ti^{4+} ions in the B-sites to realize ADPESSs with a cell volume larger than that of $La_{0.56}Li_{0.33}TiO_3$. Although the $V^{1/3}$ value increased with an increase of the substituted Zr^{4+} and Hf^{4+} ions, the logarithm of σ_b decreased linearly in contrast to the dependence of the A series.

Series C: We vaguely expected that this series might show a conductivity maximum at a $V^{1/3}$ value somewhat larger than that (i.e., $V^{1/3} \approx 387$ pm) of α-$La_{0.56}Li_{0.33}TiO_3$. This series was not the case. The logarithm of σ_b continued to increase by more than seven orders with increasing $V^{1/3}$ value. Although the slope of the log σ_b–$V^{1/3}$ plots was somewhat gentler, the $V^{1/3}$-dependence was broadly similar to that of the series A. The best bulk conductivity in this series was 5.6×10^{-4} S cm^{-1} at $x = 1$, about half of that of α-$La_{0.56}Li_{0.33}TiO_3$. Furthermore, it is worth noting that this series show a remarkably lower conductivity at the $V^{1/3}$ value of α-$La_{0.56}Li_{0.33}TiO_3$ by four orders than α-$La_{0.56}Li_{0.33}TiO_3$. This clearly demonstrates that the $V^{1/3}$ parameter is not the sole predominating factor in determining the magnitude of σ_b. The distortion of the perovskite cell took place in the sample with $x = 0$, and the conductivity was ex-

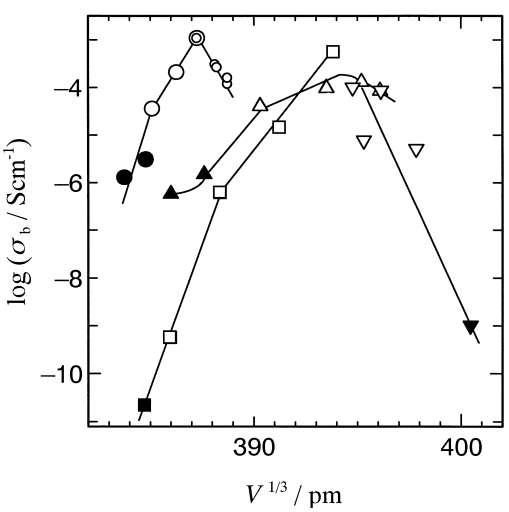

Fig. 1. Bulk ionic conductivity (σ_b) at 25°C of the Li-ADPESSs as a function of the cube roots ($V^{1/3}$) of the perovskite cell volume. Closed symbols: Li-ADPESSs with a distorted perovskite cell. ○: A series $(La_{1-x}Nd_x)_{0.56}Li_{0.33}TiO_3$; ◦: B series $La_{0.56}Li_{0.33}M(IV)_xTi_{1-x}O_3$ [M(IV) = Zr,Hf]; □: C series $(Ca_{1-x}Sr_x)_{0.56}Li_{0.33}Ta_{0.56}Ti_{0.44}O_3$; Δ: D series $(Ca_{1-x}Sr_x)_{0.56}Li_{0.33}Fe_{0.225}Ta_{0.775}O_3$; ∇: E series $Sr_{0.56}Li_{0.33}M(III)_{0.225}Ta_{0.775}O_3$ [M(III) = Cr,Fe,Co,Ga,Y].

tremely low. It was therefore determined to be of the order of 10^{-11} S cm^{-1} at room temperature by extrapolation of the conductivities above room temperature.

Series D: This series had a conductivity maximum at a $V^{1/3}$ value of about 394–395 pm. The $V^{1/3}$ value was rather larger than that of α-$La_{0.56}Li_{0.33}TiO_3$ and very close to that of $x=1$ in the series C containing Sr^{2+} ions similarly to this series.

The plot for $x=0$ did not follow the dome-shaped dependence in this series. The samples with $x=0$ exhibited no spike due to a double-layer capacitance unlike the other samples. The deviation from the dependence can be explained with a substantial contribution of electronic conduction.

Series E: Although the plots show some scatter, an overall tendency that the conductivity increases with decrease in the $V^{1/3}$ value as with the series B, can be seen from Fig. 1. The unit cell for M(|||) = Y was distorted, and its conductivity was very low, $<10^{-9}$ S cm^{-1}.

Fig. 2 shows the Arrhenius plots of the bulk conductivity for six Li-ADPESSs. Since the plots for all the Li-ADPESSs are linear, the apparent activation energies for ionic conduction and the conductivity prefactor σ_0 values are calculated and listed in Table 2.

The prefactor σ_0 changed only by a factor of 17 from 8.3×10^3 KS cm^{-1} for β-$Nd_{0.56}Li_{0.33}TiO_3$ to 1.4×10^5 KS cm^{-1} for α-$La_{0.56}Li_{0.33}TiO_3$, in spite of the large differences in σ_b. Furthermore, the σ_0 values did not show a direct correlation to the bulk conductivities. the changes in σ_0 are probably correlated to changes in the effective attempt frequency of Li^+ ions, because the parameters included in the prefactor, such as the concentrations of the Li^+ ions and vacancies and the jumping distance, can be regarded to be the same or almost the same for the Li-ADPESS prepared here, except for the effective attempt frequency. The effective attempt frequency will change reflecting various perovskite frameworks with different compositions. Nevertheless, the prefactor was found to be a less important factor than the activation energy.

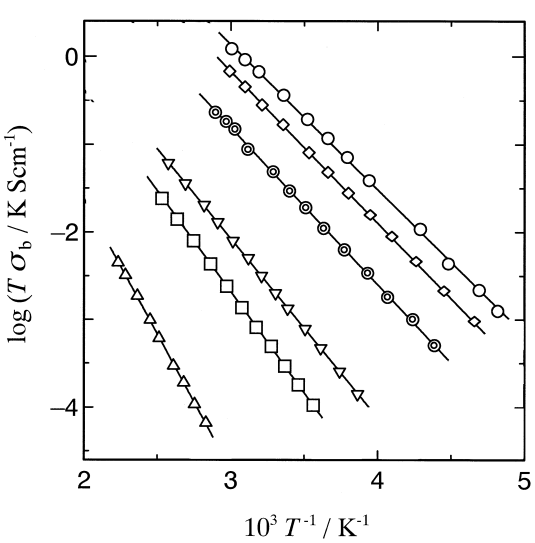

Fig. 2. Arrhenius plots of bulk ionic conductivity (σ_b) for the Li-ADPESSs: ○: α-$La_{0.56}Li_{0.33}TiO_3$; ◇: α-$Sr_{0.56}Li_{0.33}Ta_{0.56}Ti_{0.44}O_3$; ⊙: α-$La_{0.56}Li_{0.33}Hf_{0.1}Ti_{0.9}O_3$; ∇: α-$Sr_{0.56}Li_{0.33}Co_{0.225}Ta_{0.775}O_3$; □: β-$Nd_{0.56}Li_{0.33}TiO_3$; Δ: α-$(Ca_{0.7}Sr_{0.3})_{0.56}Li_{0.33}Ta_{0.56}Ti_{0.44}O_3$.

Table 2
Activation energies (ΔE) and conductivity prefactors (σ_0) for some α-Li-ADPESSs

Compositions	ΔE_{bulk} (eV)	σ_0 (KS cm^{-1})	$V^{1/3}$ (pm)
$Nd_{0.56}Li_{0.33}TiO_3$ [a]	0.46	8.3×10^3	383.7
$La_{0.56}Li_{0.33}TiO_3$	0.33	1.4×10^5	387.3
$La_{0.56}Li_{0.33}Hf_{0.1}Ti_{0.9}O_3$	0.36	3.7×10^4	388.7
$(Ca_{0.7}Sr_{0.3})_{0.56}Li_{0.33}Ta_{0.56}Ti_{0.44}O_3$	0.62	3.6×10^4	386.0
$Sr_{0.56}Li_{0.33}Ta_{0.56}Ti_{0.44}O_3$	0.34	9.9×10^4	393.8
$Sr_{0.56}Li_{0.33}Co_{0.225}Ta_{0.775}O_3$	0.41	1.1×10^4	397.8

[a] β-form with a low degree of ordering.

On the other hand, the activation energies showed a good anti-correlation to the bulk conductivities. The α-$(Ca_{0.7}Sr_{0.3})_{0.56}Li_{0.33}Ta_{0.56}Ti_{0.44}O_3$ had twice as large an activation energy as α-$La_{0.56}Li_{0.33}TiO_3$ with a similar $V^{1/3}$ value. This is responsible for the extremely low conductivity. For the most conductive α-$La_{0.56}Li_{0.33}TiO_3$ and α-$Sr_{0.56}Li_{0.33}Ta_{0.56}Ti_{0.44}O_3$, the activation energies were low and the σ_0 values were high compared with those for the others.

Looking at Fig. 1 as a whole, we can readily find out two independent log σ_b–$V^{1/3}$ dependence, which have a maximum at $V^{1/3}\approx387$ pm and at $V^{1/3}\approx395$ pm, respectively.

It is well known for β-alumina that a maximum in the self-diffusion coefficient and a minimum in the activation energy for diffusion can be found for the framework when one replaces the carrier ions by different monovalent ions in the order Li–Na–Ag–K–Rb [23]. Our results provide a good example for the reverse case that one fixes carrier ions to Li^+ ions and change the size of the framework of a conductor.

The frameworks of the Li-ADPESSs prepared here can be classified as $Ln_{0.56}$ M(IV)O_3 (most of the M(IV) ions are Ti^{4+} ions) or M(||)$_{0.56}Ta_{1-X}$[M(|||)orTi]$_X O_3$. The major constituents, M(||) and Ta ions, in the latter are less covalent than Ln^{3+} and Ti^{4+} ions in the former. In addition, the incorporation of large Sr^{2+} ions expands the perovskite cell and makes the B–O bonds a little longer. The electron density on the oxide ions in the later becomes denser; this requires a larger framework for fast ion conduction. The decrease in σ_b, namely the increase in the activation energy, is due to the repulsive interaction between Li^+ ions and the framework in the smaller side of the optimal $V^{1/3}$ value or due to the relatively strong interaction between Li^+ ions and oxide ions on one side of the loose surroundings in the larger side of the optimal $V^{1/3}$ value, as with β-alumina [23].

Acknowledgements

J.K. thanks I. Baba, O. Ohnishi and Y. Yamada (Yamakitsu System Ware, Nagoya) for building the software for ac–impedance measurements.

References

[1] A.G. Belous, G.N. Novitskaya, S.V. Polyanetskaya, Yu.I. Gornikov, Izv. Akad. Nauk SSSR., Neorg. Mater. 23 (1987) 470.
[2] Y. Inaguma, C. Liquan, M. Itoh, T. Nakamura, T. Uchida, H. Ikuta, M. Wakihara, Solid State Commun. 86 (1993) 689.
[3] H. Kawai, J. Kuwano, J. Electrochem. Soc. 141 (1994) L78.
[4] Y. Inaguma, L. Chen, M. Itoh, T. Nakamura, Solid State Ionics 70–71 (1994) 196.
[5] H. Kawai, J. Kuwano, in: P. Vincenzini (Ed.), Ceramics: Charting the Future, 3D, The proceedings of the 8th CIMTEC World Ceramic Congress Florence, Italy, June, 1994, TECHNA srl, Faenza, 1995 p. 2641.
[6] Y. Inaguma, Y. Matsui, Y. Shan, M. Itoh, T. Nakamura, Solid State Ionics 79 (1995) 91.
[7] A.D. Robertson, S.G. Martin, A. Coats, A.R. West, J. Mater. Chem. 5 (1995) 1405.
[8] A. Várez, F. Gracía-Alvarado, E. Moán, M.A. Alario-Franco, J. Solid State Chem. 118 (1995) 78.
[9] L. Fourquet, H. Duroy, M.P. Crosnier-Lopez, J. Solid State Chem. 127 (1995) 283.
[10] J.M.S. Skakle, G.C. Mather, M. Morales, R.I. Smith, A.R. West, J. Mater. Chem. 5 (1995) 1807.
[11] H. Watanabe, J. Kuwano, J. Power Sources 68/2 (1997) 416.
[12] J. Emery, J.Y. Bruzare, O. Bohnke, J.L. Fourquet, Solid State Ionics 99 (1997) 41.
[13] Y. Harada, T. Ishigaki, H. Kawai, J. Kuwano, Solid State Ionics 108 (1998) 407.
[14] Y. Harada, Y. Hirakoso, H. Kawai, J. Kuwano, Solid State Ionics, in press.
[15] Y. Inaguma, M. Itoh, Solid State Ionics 86–88 (1996) 257.
[16] Y. Inaguma, Y. Matsui, J. Yu, Y. Shan, T. Nakamura, M. Itoh, J. Phys. Chem. Solid 58 (1997) 843.
[17] J. Kuwano, A.R. West, Mater. Res. Bull. 15 (1980) 1661.
[18] A.R. Rodger, J. Kuwano, A.R. West, Solid State Ionics 15 (1985) 185.
[19] R. Kanno, Y. Takeda, O. Yamamoto, Solid State Ionics 28–30 (1988) 1276.
[20] M. Abe, Uchino, Mater. Res. Bull. 9 (1980) 147.
[21] Y. Takaki, T. Taniguchi, H. Hori, J. Ceramic Soc. Jpn. 101 (1993) 373.
[22] I.M. Hodge, M.D. Ingram, A.R. West, J. Electroanal. Chem. 74 (1976) 125.
[23] Y.Y. Yao, J.T. Kummer, J. Inorg. Nucl. Chem. 29 (1967) 2453.